ISSN 1674-1056
http://cpb.iphy.ac.cn
http://iopscience.iop.org/cpb
中国物理 B
Chinese Physics
中国物理 Chinese Physics B

Synthesis, physical properties, and annealing investigation of new layered Bi-chalcogenide $LaOBiHgS_3$

Yi Yu(于一), Chunchang Wang(汪春昌), Liang Li(李亮), Qiuju Li(李秋菊), Chao Cheng(程超), Shuting Wang(王舒婷), Changjin Zhang(张昌锦)

Citation: Chin. Phys. B . 2019, 28(1): 017401. **doi:** 10.1088/1674-1056/28/1/017401
Journal homepage: http://cpb.iphy.ac.cn; http://iopscience.iop.org/cpb

What follows is a list of articles you may be interested in

Tunneling field effect transistors based on in-plane and vertical layered phosphorus heterostructures

Shenyan Feng(冯申艳), Qiaoxuan Zhang(张巧璇), Jie Yang(杨洁), Ming Lei(雷鸣), Ruge Quhe(屈贺如歌)
Chin. Phys. B . 2017, 26(9): 097401. **doi:** 10.1088/1674-1056/26/9/097401

Thermal stability and electrical transport properties of Ge/Sn-codoped single crystalline β-Zn_4Sb_3 prepared by the Sn-flux method

Hong-xia Liu(刘虹霞), Shu-ping Deng(邓书平), De-cong Li(李德聪), Lan-xian Shen(申兰先), Shu-kang Deng(邓书康)
Chin. Phys. B . 2017, 26(2): 027401. **doi:** 10.1088/1674-1056/26/2/027401

Structural stabilities and electrical properties of $Ba_8Ga_{16-x}Cu_xSn_{30}$ single crystals under high temperatures

Jin-Song Wang(王劲松), Feng Cheng(程峰), Hong-Xia Liu(刘红霞), De-Cong Li(李德聪), Lan-Xian Shen(申兰先), Shu-Kang Deng(邓书康)
Chin. Phys. B . 2016, 25(6): 067402. **doi:** 10.1088/1674-1056/25/6/067402

Critical current density behaviors across a grain boundary inclined to current with different angles in $YBa_2Cu_3O_{7-\delta}$ bicrystal junctions

Tao Hua(花涛), Wei-Wei Xu(许伟伟), Zheng-Ming Ji(吉争鸣), Da-Yuan Guo(郭大元), Qing-Yun Wang(王青云), Xiang-Rong Ma(马湘蓉), Rui-Yu Liang(梁瑞宇)
Chin. Phys. B . 2016, 25(6): 067401. **doi:** 10.1088/1674-1056/25/6/067401

Sn-based type-VIII single-crystal clathrates with a large figure of merit

Deng Shu-Kang, Li De-Cong, Shen Lan-Xian, Hao Rui-Ting
Chin. Phys. B . 2012, 21(1): 017401. **doi:** 10.1088/1674-1056/21/1/017401

Synthesis, physical properties, and annealing investigation of new layered Bi-chalcogenide $LaOBiHgS_3$*

Yi Yu(于一)[1,†], Chunchang Wang(汪春昌)[1], Liang Li(李亮)[2], Qiuju Li(李秋菊)[1], Chao Cheng(程超)[2], Shuting Wang(王舒婷)[1], and Changjin Zhang(张昌锦)[3]

[1] *School of Physics and Material Science, Anhui University, Hefei* 230601, *China*

[2] *Institute of Physical Science and Information Technology, Anhui University, Hefei* 230601, *China*

[3] *High Magnetic Field Laboratory, Chinese Academy of Sciences and University of Science and Technology of China, Hefei* 230026, *China*

(Received 9 September 2018; revised manuscript received 15 October 2018; published online 25 December 2018)

The transport and thermoelectric properties together with annealing of the new layered Bi-chalcogenide $LaOBiHgS_3$ are studied. On the transport part, the insulating behavior of the as-grown sample is evidently depressed by post annealing. A hump-like abnormality appears around 170 K. The thermoelectric performance of the sample is observably improved by the annealing, mainly because of the enhanced electrical conductance. The present results suggest that the physical properties of $LaOBiHgS_3$ are sensitive to post annealing and the possible micro adjustments that follow, indicating the layered Bi-chalcogenide family to be an ideal platform for designing novel functional materials.

Keywords: thermoelectric material, Bi-chalcogenide, post annealing

PACS: 74.25.F–, 74.62.En, 74.20.Rp, 74.70.Xa **DOI:** 10.1088/1674-1056/28/1/017401

1. Introduction

The search for and exploitation of new sustainable energy sources have always been the focus of attention for human society, especially in the present circumstances, as the traditional nonrenewable energy sources are becoming increasingly exhausted. Amongst the many options, thermoelectric devices, i.e., devices that convert thermal energy into electrical energy, have been favored for their high stability, long service life, and zero release of greenhouse gases. To have the technique widely utilized in social and industrial activities, practical thermoelectric materials with high efficiency are desirable.

Not long ago, promising thermoelectric properties were discovered in the BiS_2-based layered material.[1–5] With the simple layered structure of alternating conducting BiS_2 layers and various insulating layers, the electronic structure and physical properties could be effectively tuned by element doping or intercalation.[6] The thermoelectric performance is usually judged by the dimensionless figure of merit (ZT), with the definition of $ZT = S^2T/\rho\kappa$, where S, T, ρ, and κ are the Seebeck coefficient, temperature, electrical resistivity, and thermal conductivity, respectively. As the Seebeck effect coefficient and thermal transport properties are influenced by both phonon and carrier behaviors,[2,7,8] it is beneficial to promote the carrier mobility and suppress the thermal conductivity to enhance ZT. Take $LaOBiS_2$ for example, S-site Se doping increases the in-plane chemical pressure and promotes the carrier mobility.[3,5,9] Therefore, a high ZT value of 0.36 was obtained in LaOBiSSe at 650 K, which is the highest ZT recorded in this series.[5]

Recently, compounds of further intercalation to $LaOBiS_2$ were under intense study. $LaOBiPbS_3$ is one of them, with the rock-salt PbS cubic inserted into the two layered BiS_2 conducting layers.[1,9] By means of synchrotron x-ray diffraction and neutron diffraction, $LaOBiPbS_3$ was confirmed to own the 4-layer-type conducting layer. The structure is similar to that of the Bi_4Te_6 conducting layers in $CsBi_4Te_6$, another member of the Bi-chalcogenide family.[11] The narrow gap semiconductor ($\sim$ 100 meV) satisfies both large S and small ρ,[7] which offers good potential for practical application. However, more compounds with various compositions and electronic properties have to be tried out in the series, to obtain a practical thermoelectric material with better performance. In this work, we report the successful synthesis of the $LaOBiHgS_3$ compound, the iso-structure counterpart of $LaOBiPbS_3$. The basic physical properties and effects of vacuum annealing are also displayed and comprehensively discussed.

2. Experiment

Polycrystalline samples of $LaOBiHgS_3$ were prepared via the solid-state reaction method. High-purity powder of La_2S_3, La_2O_3, Bi, Bi_2S_3, and HgS were weighed strictly according to the stoichiometric ratio in a glove box filled with inert gas. The mixture was thoroughly ground, pelletized, and sealed into an evacuated quartz tube (below 2×10^{-5} Pa) before it was heated at 940 K for 25 hours. The sintering process was conducted

*Project supported by the National Natural Science Foundation of China (Grant Nos. 51572001, 11404002, and 11404003) and the '211 Project' of Anhui University, China (Grant No. J01001319J10113190007).

†Corresponding author. E-mail: onlyyuyi@mail.ustc.edu.cn

© 2019 Chinese Physical Society and IOP Publishing Ltd

in ambient pressure. The obtained sample was ground and pelletized again in the inert gas atmosphere for homogenization, and sintered at 1020 K in vacuum quartz tubes for another 25 hours. The annealed samples were selected from the same batch as the as-grown ones. They were heated up to 673 K in vacuum quartz tubes for 6 hours before taking out. The obtained as-grown samples were characterized by powder x-ray diffraction (XRD) utilizing $K\alpha 1$ radiation. The actual composition of the crystal was determined using x-ray photoelectron spectroscopy (XPS) carried out on an x-ray photoelectron spectrometer (ESCALAB 250Xi, Thermo, USA). The dc electrical resistivity measurement was performed using a standard four-probe method with a constant current of 1 mA on the Quantum Design physical properties measurement system (PPMS) from 2 K to 300 K. The electrical resistivity and Seebeck coefficient at higher temperatures were measured simultaneously by a commercial equipment (ULVAC-RICO: ZEM-3, Japan) under He atmosphere. The error bar of the data for either PPMS-9 or ZEM-3 is less than 1%.

3. Results and discussion

In order to determine the crystal structure of the as-grown samples, bulks of crystals are chosen and ground to fine powders for the powder XRD measurements. The XRD patterns are displayed in Fig. 1. The diffraction peaks of $LaOBiHgS_3$ are in accordance with those of $LaOBiPbS_3$,[1,10] revealing the tetragonal crystal structure (space group: *P*4/*nmm*). Tiny extra peaks of impurity phase of HgS are also detected. By using the software of XRD-program, we take a general fit to the XRD data and determine the lattice constants as $a = 4.06$ Å and $c = 19.86$ Å. Considering the smaller radius of Hg compared to that of Pb, the shrinkage of the *ab*-plane lattice parameter compared to $LaOBiPbS_3$ (4.0982 Å)[10] is comprehensible. XPS measurements of three bulk samples from the same batch are performed, giving the average element ratio to be La:Bi:Hg:S = 1.00(3):1.09(6):0.96(5):3.12(1), as shown in Table 1. The oxygen content cannot be determined accurately by XPS because of the adhering oxygen and water molecules on the sample surface. The actual Hg ratio is relatively lower than the nominal one, which is attributed to the high effumability of the element.

The temperature dependence of the resistivity for $LaOBiHgS_3$ is displayed in Fig. 2 in the temperature range of 2–300 K. The parent compound exhibits typical insulating transport behavior as temperature descends. The resistivity goes beyond the resistance measuring limits of the PPMS below 95 K. While as shown in the inset of Fig. 2, $\rho(T)$ of the post annealed $LaOBiHgS_3$ sample undergoes drastic depression in the whole temperature region. The ρ of the annealed sample is only 4.5 Ω·mm at room temperature, nearly three orders lower in magnitude than that of the as-grown one. A hump-like abnormality is observed at around 170 K in the ρ–T relation of the annealed sample, below which the $\rho(T)$ behavior appears metallic. The observation of a similar hump feature was also reported in $A_xFe_{2-y}Se_2$ (A = K, Rb, Cs, and Tl) single crystals,[12,13] where superconductivity was developed from AFM Mott insulator with a rather high Néel temperature.[13,14] The abnormal detected in the $A_xFe_{2-y}Se_2$ superconductors was interpreted to be caused by phase coexistence and competitions.

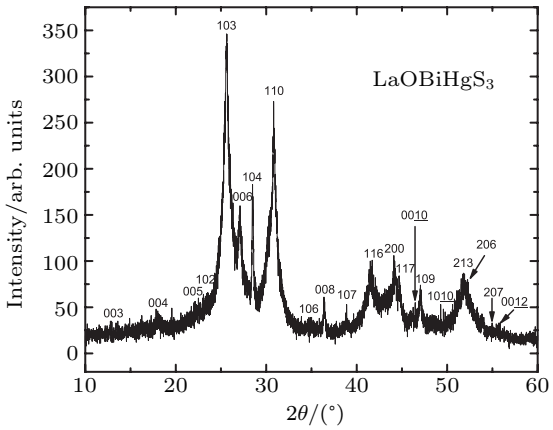


Fig. 1. Powder x-ray diffraction pattern of the as-grown $LaOBiHgS_3$ sample.

Table 1. Element ratio of the $LaOBiHgS_3$ sample determined by XPS.

	La	Bi	Hg	S
1	1.00(3)	1.09(2)	0.98(2)	3.09(6)
2	1.00(2)	1.11(3)	0.96(2)	3.15(5)
3	1.00(3)	1.08(3)	0.95(1)	3.11(3)
Average	1.00(3)	1.09(6)	0.96(5)	3.12(1)

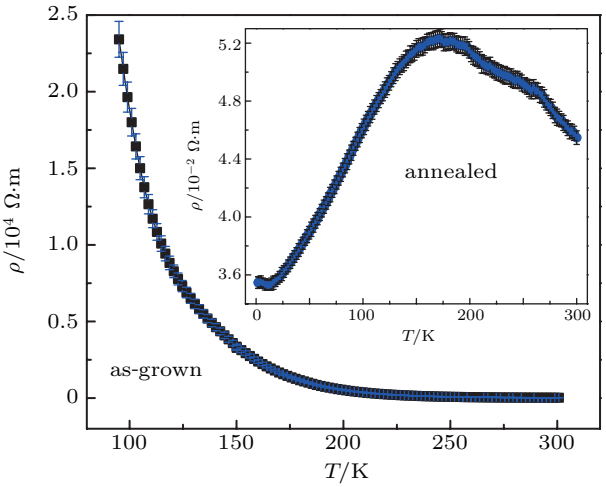


Fig. 2. Temperature dependence of resistivity of the as-grown $LaOBiHgS_3$ sample from 2 K to 300 K. The inset displays the temperature dependence of resistivity of the annealed $LaOBiHgS_3$ sample. Error bars are amplified 1000 times.

To evalue the thermoelectric performance of $LaOBiHgS_3$, the temperature dependence of the electrical resistivity and Seebeck coefficient was measured from 300 K to 770 K for the as-grown and the annealed samples, as shown in Figs. 3(a)

and 3(b), respectively. The negative sign of S indicates that the main contributing carriers are electrons. As one can see, the behavior of the absolute value of S ($|S|$) undergoes a similar evolution in the two cases. Both $|S|$ values increase with rising temperature below 665 K, followed by steep drops with different descending rates. Other than the $S(T)$ behavior, drastic contrast is observed between the ρ–T curves. For the as-grown sample, ρ decreases monotonously in the whole temperature range, and the decrease becomes slow and steady above 416 K. While for the post annealed sample, ρ increases with ascending temperature overall, and the growing rate becomes almost constant above 600 K. Generally speaking, the thermal conductivity of the Bi-chalcogenides moderately increases with ascending temperature. For convenience, the thermoelectricity is more often estimated by the power factor (PF), defined as PF $= S^2\sigma$. Figure 3(c) gives the temperature dependence of the PF value for the as-grown and the annealed samples, respectively. PF of the as-grown sample is evidently enhanced by the rising temperature. Due to the temperature limit of the device, the maximum of PF values reaches 0.125 $\mu W/cm \cdot K^2$ for the as-grown sample at 770 K, an order of magnitude smaller compared to that of $LaOBiPbS_3$ (around 1.18 $\mu W/cm \cdot K^2$ at 770 K).[15] A peak appears in the PF–T curve of the annealed sample around 665 K, with the PF value of 0.339 $\mu W/cm \cdot K^2$, which is three times larger compared to that of the as-grown sample at the same temperature. As could be observed from Figs. 3(a) and 3(b), the $|S|$ value does not differ much after the annealing. Thus, the enhancement of the thermoelectric performance mainly results from the fierce depression of the $\rho(T)$ value.

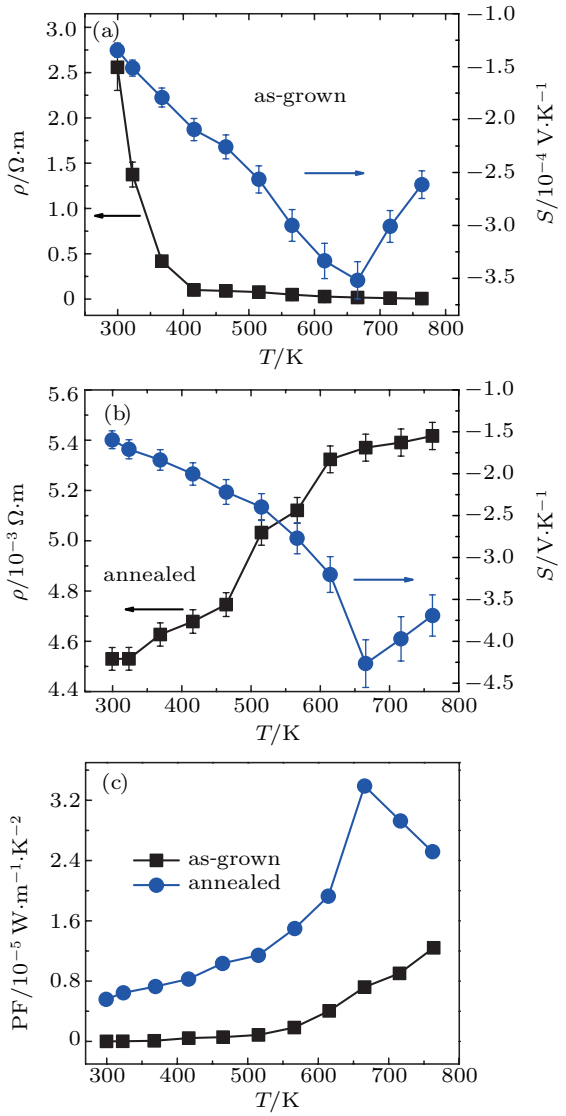


Fig. 3. Temperature dependence of the resistivity and Seebeck coefficient from 300 K to 770 K for (a) the as-grown and (b) the annealed $LaOBiHgS_3$ samples. Error bars are amplified by 100 times. (c) Temperature dependence of the thermoelectric power for the as-grown and the annealed $LaOBiHgS_3$ samples.

To comprehend the transport transformation of the $LaOBiHgS_3$ sample after annealing, it is beneficial to discuss the effects of different ways of post annealing. Oxygen annealing has been widely utilized in tuning the chemical composition and local physical properties, where removable oxygen atoms are intercalated into the compound during the process. Take the $FeTe_{1-x}S_x$ superconductors for instance, the as-grown sample is often non-superconducting because of the excess iron. As mentioned in previous reports, the exchange field of the local ferromagnetic interaction breaks the cooper-pairs, and depresses the superconductivity.[12] While the oxygen intercalated during the annealing process could effectively suppress the local magnetic moment, and therefore, introduces superconductivity.[16,17] It should be mentioned that the extra dose of oxygen is often removable via post vacuum annealing, rendering the $FeTe_{1-x}S_x$ superconducting crystals reentering the normal state.

On the other hand, the effects of vacuum annealing are much more diversified. As in the present case, the evident suppression of the insulating behavior might be caused by the complex effects of different factors, and possible reasons are proposed as follows. Firstly, from the perspective of composition change, the increase of the oxygen vacancy (V_O) density at high temperatures should not be excluded from consideration. As is well known, V_Os play a crucial role in tuning the physical properties of oxides. In the present sample, as shown in Fig. 2, the increase of V_Os would serve as extra carriers, enhancing the carrier density and the electrical conductance. In this scenario, the annealed sample of $LaOBiHgS_3$ would be a dual carrier system, and the electrical conduction is contributed by both electron carriers and ionic carriers. Secondly, former study on the TiO_2 ceramic reveals that at temperatures high enough, the V_Os would be thermally delocalized and obtain high mobility. Further on, to lower the summation of interactive energies, V_Os tend be become ordered, and a fragile conductive filament could be formed during the annealing process that drastically reduces the electrical resistance. Thirdly, micro-structure adjustments[17,18] and further homogenization

of the element distributions[19] are often observed during vacuum annealing. Annealing usually leads to the shrinkage of the lattice parameters, which directly increases the orbital overlapping, and therefore, enhances the electrical conducting. Similar behavior was also detected in the case of Se element substitution in $LaOBiS_{2-x}Se_x$,[3,9] which could be viewed as the parent compound of $LaOBiHgS_3$ before intercalation.

4. Conclusion

To summarize, we have successfully synthesized a new layered Bi-chalcogenide polycrystal $LaOBiHgS_3$. Through XRD measurement, the crystal structure of $LaOBiHgS_3$ is determined to be categorized into the tetragonal *P*4/*nmm* space group, which is similar to that of $LaOBiPbS_3$. The as-grown sample displays typical insulating behavior, and a relatively low thermoelectric performance, with the PF value growing monotonously with ascending temperature above 300 K. By post vacuum annealing, the resistivity is reduced by three orders in magnitude at room temperature, and a hump-like abnormal appears around 170 K. The PF maximum is enhanced observably, reaching 0.339 $\mu W/cm \cdot K^2$ at around 665 K. Further decrease of the lattice parameter and increase of the orbital overlapping should be an effective strategy to enhance the thermoelectric properties of the layered Bi-chalcogenide material.

References

[1] Sun Y L, Ablimit A, Zhai H F, Bao J K, Tang Z T, Wang X B, Wang N L, Feng C M and Cao G H 2014 *Inorg. Chem.* **53** 11125

[2] Omachi A, Kajitani J, Hiroi T, Miura O and Mizuguchi Y 2014 *J. Appl. Phys.* **115** 083909

[3] Mizuguchi Y, Omachi A, Goto Y, Kamihara Y, Matoba M, Hiroi T, Kajitani J and Miura O 2014 *J. Appl. Phys* **116** 163915

[4] Nishida A, Nishiate H, Lee C H, Miura O and Mizuguchi Y 2016 *J. Phys. Soc. Jpn.* **85** 074702

[5] Nishida A, Miura O, Lee C H and Mizuguchi Y 2015 *Appl. Phys. Express* **8** 111801

[6] Mizuguchi Y 2015 *J. Phys. Chem. Solids* **84** 34

[7] Bulusua A and Walker D G 2008 *Superlattices Microst.* **44** 1

[8] Yu Y, Wang C C, Li Q J, Cheng C, Wang S T and Zhang C J 2018 *Ceram. Int.* **45** 817

[9] Mizuguchi Y, Miura A, Kajitani J, Hiroi T, Miura O, Tadanaga K, Kumada N, Magome E, Moriyoshi C and Kuroiwa Y 2015 *Sci. Rep.* **5** 14968

[10] Mizuguchi Y, Hijikata Y, Abe T, Moriyoshi C, Kuroiwa Y, Goto Y, Miura O, Lee S, Torii S, Kamiyama T, Lee C H, Ochi M and Kuroki K 2017 *Europhys. Lett.* **119** 26002

[11] Chung D Y, Hogan T, Brazis P, Rocci-Lane M, Kannewurf C, Bastea M, Uher C and Kanatzidis M G 2000 *Science* **287** 1024

[12] Yu Y, Zhang C J, Tong W, Zhang L, Tan D, Pi L, Yang Z R, Tian M L, Tan S and Zhang Y H 2012 *New J. Phys.* **14** 023032

[13] Fang M H, Wang H D, Dong C H, Li Z J, Feng C M, Chen J and Yuan H Q 2011 *Europhys. Lett.* **94** 27009

[14] Yan X W, Gao M, Lu Z Y and Xiang T 2011 *Phys. Rev. Lett.* **106** 087005

[15] Mizuguchi Y, Nishida A, Omachi A and Miura O 2016 *Cogent Physics* **3** 1156281

[16] Mizuguchi Y, Deguchi K, Kawasaki Y, Ozaki T, Nagao M, Tsuda S, Yamaguchi T and Takano Y 2011 *J. Appl. Phys.* **109** 013914

[17] Noji T, Suzuki T, Abe H, Adachi T, Kato M and Koike Y 2010 *J. Phys. Soc. Jpn.* **79** 084711

[18] Yu Y, Shao J F, Tan S, Zhang C J and Zhang Y H 2013 *J. Phys. Soc. Jpn.* **82** 034718

[19] Taen T, Tsuchiya Y, Nakajima Y and Tamegai T 2009 *Phys. Rev. B* **80** 092502